Article:
Islam, KMA, Gani Adnan, MS, Zannat, KE et al. (2022) Spatiotemporal dynamics of NO2 concentration with linear mixed models: A Bangladesh case study. Physics and Chemistry of the Earth, 126. 103119. p. 103119. ISSN: 1474-7065

https://doi.org/10.1016/j.pce.2022.103119

Spatiotemporal dynamics of NO_2 concentration with linear mixed models: a Bangladesh case study

K. M. Ashraful Islam[1], Mohammed Sarfaraz Gani Adnan[1,2], Khatun E Zannat[1,3], Ashraf Dewan[4]

[1]Department of Urban and Regional Planning, Chittagong University of Engineering and Technology (CUET), Chattogram 4319, Bangladesh

[2]Environmental Change Institute, School of Geography and the Environment, University of Oxford, OX1 3QY, United Kingdom

[3]Choice Modelling Centre (CMC), Institute for Transport Studies (ITS), University of Leeds, LS2 9JT, Leeds, United Kingdom

[4]Spatial Sciences Discipline, School of Earth and Planetary Sciences, Curtin University, Perth 6102, Australia

Abstract

There is currently a limited understanding of how climatic and anthropogenic factors affect atmospheric NO_2 concentration, and how these factors are associated with air pollution over space and time. Using high-resolution TROPOMI satellite data, this study estimates both the degree of association between climatic and anthropogenic factors, and the spatiotemporal variability of NO_2 concentration over Bangladesh. Several linear mixed models were developed to isolate possible factors affecting the NO_2 concentration values recorded between July 2018 and June 2019). This included monthly mean maximum temperature (MMAXT), rainfall, wind speed (WS), relative humidity (RH), enhanced vegetation index (EVI), population density, and distance from industrial activities. The study revealed that the very urbanized central region of Bangladesh experienced high NO_2 concentrations, particularly from September through to March. Dynamic variables such as RH, MMAXT, RAIN, and WS can positively or negatively influence NO_2 depending on the time of year. Areas with a high vegetation cover, a low population density, and located some distance from industrial areas tended to have low NO_2 concentrations. This study concluded that policy measures such as transboundary air quality agreements, the introduction of a month-specific green tax, decentralization, industrial relocation, and increased urban tree plantation activities could all prove valuable in reducing NO_2 pollution in Bangladesh.

Key words Air pollution; NO_2 concentration; TROPOMI; linear mixed model; remote sensing; Bangladesh

1. Introduction

Air pollution is one of the main causes of premature deaths in human populations (Cooper et al., 2020). In 2012, approximately seven million people died due to diseases associated with air pollution: one in eight of the total fatalities across the world in that year (WHO, 2014). Many policies and strategies at the global, regional, and local levels have been formulated to ensure environmental sustainability and healthy living by reducing pollution concentrations (Melamed et al., 2016). Nitrogen dioxide (NO_2) is recognized as a significant pollutant by both the World Health Organization (WHO) and the United States Environmental Protection Agency (US EPA) (Herron-Thorpe et al., 2010; Melamed et al., 2016). Various natural and anthropogenic factors are responsible for emitting NO_2 into the air. This includes chemical reactions due to lightning, soil emission, industrial and vehicular burning of fossil fuel, use of natural gas without an outlet, kerosene, liquified petroleum gas (LPG) apparatus, tobacco, and wood-burning, (Spicer et al., 1993; Zhu et al., 2019). Consistent exposure to NO_2 can cause various health hazards such as cardiovascular disease, lung cancer, and other life-threatening respiratory diseases (Atkinson et al., 2018). A recent study had also noted a positive correlation between atmospheric NO_2 and risks of COVID-19 infection (Zhu et al., 2020).

Various environmental policies have been enacted in many countries to reduce NO_2 levels and attempt to lessen the societal costs associated with these emissions (Ryu et al., 2019). Ongoing monitoring and characterization of NO_2 concentrations are considered to be fundamental in any air pollution exposure assessment work and associated environmental policy formulation (Bechle et al., 2013; Li et al., 2020). NO_2 has a short photochemical lifetime: 2 to 5 hours during the daytime in summer and 12 to 24 hours during winter (Goldberg et al., 2021). The highly variable nature of emission sources means the distribution of this pollutant varies both spatially and temporally (Cooper et al., 2020; Goldberg et al., 2021). High-quality in-situ measurements allow an accurate assessment of NO_2; however, a lack of such measurement capability is evident in many developing countries (Bechle et al., 2013). The limited number of monitoring stations usually found in these countries usually results in a poor understanding of the actual spatiotemporal distribution (Lee and Koutrakis, 2014; Zhu et al., 2019). This can result in the formulation of environmental policies based on inadequate information, and can actually enhance disease burdens. The collection and use of accurate information is vital in supporting informed decision-making.

Advances in remote sensing technology now enable researchers to efficiently trace atmospheric NO_2 (Bechle et al., 2013; Zhu et al., 2019). Many studies now routinely use satellite data to monitor spatiotemporal changes of tropospheric NO_2 (Biswal et al., 2020; Georgoulias et al., 2019; Ryu et al., 2019; Shah et al., 2020; Wang et al., 2019; Xu et al., 2020; Zheng et al., 2018). The data allows the

assessment of long-term pollution trends, mapping at ungauged locations, prediction of future air quality scenarios and the detection of extreme air pollution events (Duncan et al., 2014). Currently, the European Remote Sensing (ERS-2) Global Ozone Monitoring Experiment (GOME), Envisat SCanning Imaging Absorption SpectroMeter for Atmospheric CHartographY (SCIAMACHY), NASA's Aura Ozone Monitoring Instrument (OMI), and Exploitation of Meteorological Satellites (EUMETSAT) Metop-A (GOME-2) (Duncan et al., 2014) are available to map and monitor NO_2. The latest tropospheric vertical column of NO_2 data provided by the European Space Agency's (ESA) Sentinel 5P (commonly known as the TROPOspheric Monitoring Instrument (TROPOMI)) (ESA, 2018) accurately estimates NO_2 emission values when compared with actual in-situ data recordings (Goldberg et al., 2021; Lorente et al., 2019; Omrani et al., 2020). The TROPOMI spectrometer has been collecting NO_2 information since October 2017. The high spatiotemporal resolution and improved sensitivity and accuracy of TROPOMI datasets make them very useful in examining atmospheric NO_2 over time and space when compared to previous satellite instrumentation suites (Dix et al., 2020; Goldberg et al., 2021). As a result, its use in monitoring emission products such as NO_2 is increasing globally (Cooper et al., 2020; Dix et al., 2020; Goldberg et al., 2021; Shikwambana et al., 2020; Wu et al., 2021). Satellite overpass times differ between latitudes, so global-scale NO_2 studies may be of little use in developing policies to curb increases in air pollution in a country experiencing a rapid growth of industries and anthropogenic activities (Bechle et al., 2013).

The use of robust, spatial and temporal modeling is essential in any investigations of regional NO_2 pollution, and is critical in helping decision-makers formulate appropriate environmental policies (Vîrghileanu et al., 2020). Accurately analyzing the amount of atmospheric trace gases present at a location is important in characterizing air pollution (Aggarwal and Toshniwal, 2019; Cichowicz et al., 2017; Nemet et al., 2010). As with other air quality indicators, the relative level of NO_2 present is generally associated with a set of complex weather parameters (Davis and Kalkstein, 1990). Local and regional climate also play an important role in the spatial and temporal variability of this gas (Elminir, 2005). Anthropogenic factors such as industrial emission and population density, as well as the extent of vegetation cover, can also influence NO_2 pollution patterns (Zhu et al., 2019).

Many studies have focused on diagnosing NO_2 concentrations using various combinations of explanatory variables and modeling approaches. Statistical modeling approaches include the use of cokriging (Ryu et al., 2019), geographically weighted regression (GWR) (Zheng et al., 2019), linear regression (ul-Haq et al., 2018), land use regression (LUR) (Lee and Koutrakis, 2014; Novotny et al., 2011), and linear mixed model (LMM) (Lee and Koutrakis, 2014). Machine learning techniques such as Random Forest (RF) (Zhu et al., 2019), support vector machines (SVM), artificial neural

networks (ANN) (Juhos et al., 2008), and space-time neural network (Li et al., 2020) are also used for measuring tropospheric NO_2. Studies indicate that LMM has better predictive power in explaining spatial and temporal NO_2 distribution as compared to classical linear regression approaches, e.g., multivariate model (Lee et al., 2011; Lee and Koutrakis, 2014). Though a linear regression model can establish an empirical relationship between dependent and independent variables, it disregards the variation among groups (e.g., month) (El-Assi et al., 2017). On the other hand, LMM considers grouping/clustering of variables; enabling a better understanding of the temporal changes of a dependent variable (Gelman and Hill, 2006; Magezi, 2015). The LMM application does, however, appear to have limited capability in regards the mapping and modeling of NO_2 concentrations (Lee and Koutrakis, 2014).

Various studies have measured the concentration of atmospheric NO_2 in different geographical settings over time and space (Herron-Thorpe et al., 2010; Ryu et al., 2019; ul-Haq et al., 2018), however the majority of them have incorporated only a few factors in the modelling (Elminir, 2005; Zhou et al., 2012). Only a small number of studies have focused specifically on developing countries where station-based NO_2 monitoring data is notably lacking (Azkar et al., 2012; Bechle et al., 2013). In these circumstances a comprehensive evaluation of NO_2 is difficult to perform due to (i) lack of station-based data (Bechle et al., 2013; Liu et al., 2016); (ii) spatial heterogeneity of the pollutant (Cooper et al., 2020; Goldberg et al., 2021); (iii) uncertainties in various statistical and machine learning-based models (Li et al., 2020; Zhang et al., 2016); and (iv) a lack of robust spatiotemporal modeling approaches (Bechle et al., 2013; Vîrghileanu et al., 2020). The aim of this research, using Bangladesh as the case study area, is twofold: (i) to model spatiotemporal distribution of NO_2 concentration with high-resolution TROPOMI data; (ii) to isolate factors affecting its distribution through the use of spatial linear mixed models (LMMs).

2. Materials and methods

2.1. NO_2 pollution in Bangladesh

Bangladesh is located between latitude 20º34′ and 26º38′ N, and longitude 88º01′ and 92º41′ E in South Asia (Figure 1) and has a population of 164.6 million people (BBS, 2019). The climate regime is sub-tropical, with persistent humidity and precipitation controlled by a monsoonal season (Mullick et al., 2019). The major cities are Dhaka, Chittagong, Rajshahi, Sylhet, Khulna, and Barisal. Ever-increasing city populations, as well as essentially uncontrolled urbanization, has resulted in many environmental issues. This includes heavy traffic congestion and severe air pollution (Rana and Khan, 2020). Almost 33% of total population of the country lives in cities, with a 2.92% decadal growth of urban population (DoE, 2018).

Bangladesh is considered one of the most polluted countries in the world (Kurata et al., 2020). Every year, it experiences a loss of approximately 200–800 million US$ due to air pollution, especially in the major cities (Azkar et al., 2012). Emissions from motor vehicles and industrial discharges are major sources of such pollution (Islam et al., 2020). The level of pollution is increasing every year, so damage to lives and resources has become a common feature. As a result, the country is struggling to meet widely accepted, WHO-defined air quality standards (Rana and Khan, 2020). Researchers commonly employ discrete methods to produce various air pollution scenarios. Salam et al. (2008) used in-situ observations to measure the distribution of gaseous pollutants in Dhaka city. To simulate the severity of air pollutants in Bangladesh, Azkar et al. (2012) used Weather Research and Forecasting (WRF) – Community Multiscale Air Quality Model (CMAQ) model, incorporating data from a limited number of stations. Sadia et al. (2019) measured $PM_{2.5}$ and NO_2 concentrations in Dhaka using five locations. Rahman et al. (2019) used data from three monitoring stations to assess trace gases during different seasons. Islam et al. (2019) utilized OMI data to measure aerosol optical properties for more than 15 years. A recent study employed TROPOMI data to evaluate changes in four air pollutants (e.g., NO_2, SO_2, CO, and O_3) in regard COVID-19 lockdown policies (Rahman et al., 2020).

There were only 11 Department of Environment (DoE) air quality monitoring stations operating in Bangladesh from 2012 to June 2019. The accurate observation of NO_2 concentration is, therefore, very challenging (Azkar et al., 2012; DoE, 2018). Existing studies have used only a specific city, or a few sampling locations, to evaluate NO_2 pollution (Rahman et al., 2019; Sadia et al., 2019), meaning that studies on spatiotemporal patterns of NO_2 concentration at the national level, in relation to anthropogenic and environmental factors, are few and far between. Existing studies could also not quantify temporal variations in NO_2 pollution (ul-Haq et al., 2018) due to the absence of high-resolution data. This study attempts to rectify these shortcomings.

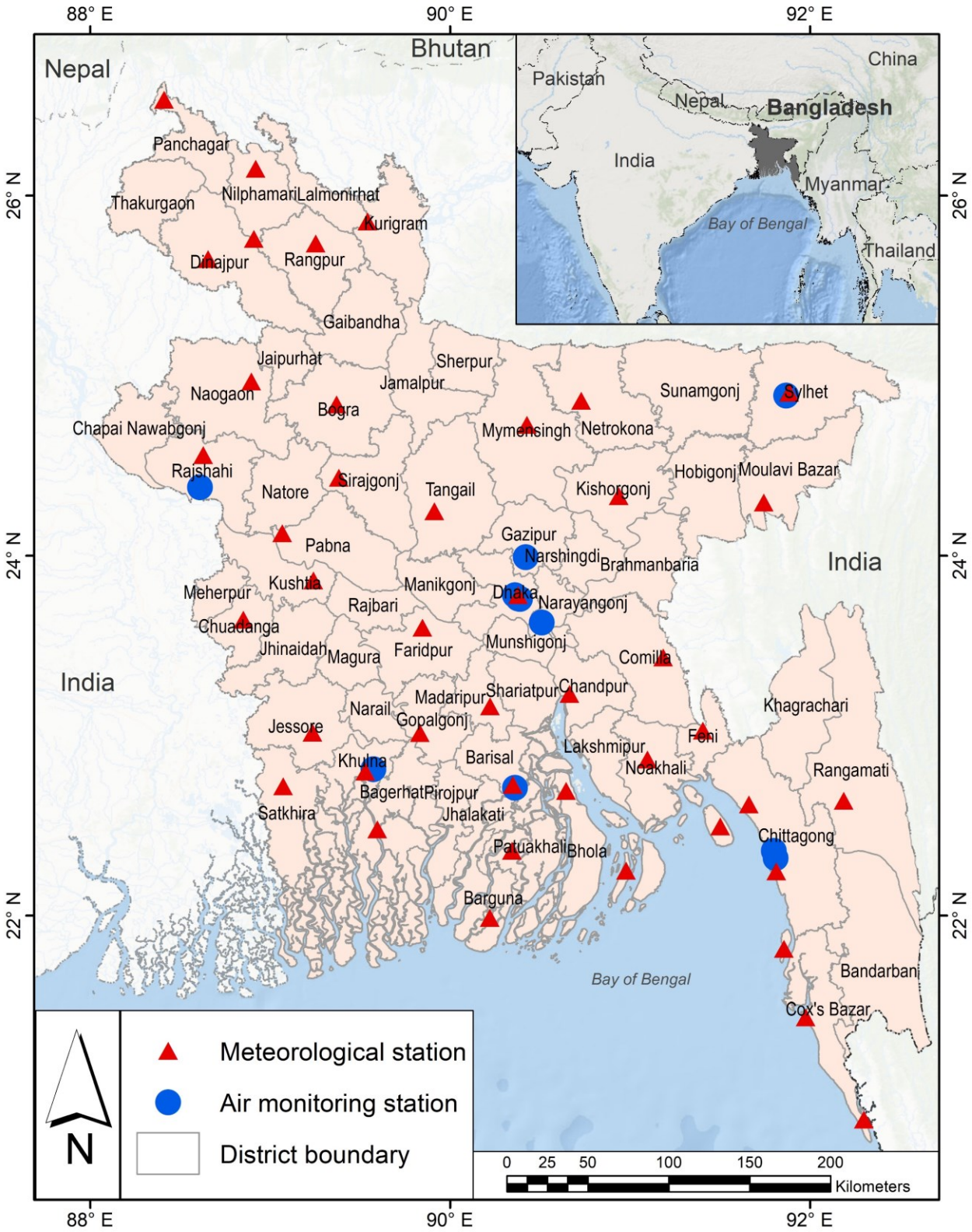

Figure 1 Location of air quality and meteorological measurement stations in Bangladesh

2.2. TROPOMI data

This study used Sentinel 5P TROPOMI data to monitor spatial and temporal variations of NO_2 concentration. The tropospheric vertical column density (VCD) dataset of NO_2 was obtained through the Google Earth Engine (GEE) platform (Gorelick et al., 2017). The dataset has a spatial resolution of 0.01 arc-degree. This study utilized preprocessed level 3 (L3) products, which were produced by Quality Assurance (QA) filtering (pixels with QA value <75% were removed) (Eskes et al., 2019). The L3 NO_2 VCD data for 12 months (July 2018 - June 2019) were retrieved, based on periods common to both TROPOMI and the in-situ NO_2 data. TROPOMI NO_2 data are available for different times of the day. A reducer function was used (JavaScript code) in the GEE platform to batch-process time-series data for a month. This was then aggregated to derive the mean monthly VCD of NO_2. In this function, a scale argument was used for co-registering all monthly grids. The images were subsequently exported to GeoTIFF for further analyses.

Table 1 Datasets used in this study

Variable	Resolution	Unit	Data source
Tropospheric NO_2 vertical column density	0.01 arc degree	mol/m^2	Sentinel-5 Precursor Offline *https://scihub.copernicus.eu/*
Ambient NO_2 concentration	-	ppb	Department of Environment (DoE), Bangladesh *http://case.doe.gov.bd/*
Enhanced vegetation index (EVI)	1 km	-	MOD13A2 *https://lpdaac.usgs.gov/products/mod13a2v006/*
Windspeed	2.5 arc minutes	m/s	Monthly Climate Grid *http://www.climatologylab.org/terraclimate.html*
Rainfall amount	0.1 arc degrees	mm/hr	Global precipitation measurement (GPM) (v6) *https://disc.gsfc.nasa.gov/datasets/GPM_3IMERGM_06/summary*
Maximum temperature	-	^oC	Bangladesh Meteorological Department (BMD) *http://live3.bmd.gov.bd/*
Relative humidity	-	%	Bangladesh Meteorological Department (BMD) *http://live3.bmd.gov.bd/*
Population density	3 arc second	people/grid	WorldPop Global Project Population Data *https://www.worldpop.org/*
Location of industrial activity	-	-	HOTOSM Bangladesh Buildings *https://www.hotosm.org/* *https://data.humdata.org/dataset/hotosm_bgd_buildings*

2.3. In-situ data

Many studies have reported a strong correlation between satellite and ground-based NO_2 observations (Bechle et al., 2013; Li et al., 2020; Tzortziou et al., 2018). A short photochemical life makes atmospheric NO_2 strongly associated with local emissions caused by anthropogenic forcing (Goldberg et al., 2021). For this study, air quality observation data from 11 monitoring stations was obtained from the Department of Environment (DoE) of Bangladesh and used to estimate the degree of alignment between the terrestrial and in-situ observations. The DoE had previously installed air quality monitoring stations across the country (Figure 1) as part of the Clean Air and Sustainable Environment (CASE) project. Three monitoring stations were located in Dhaka, two were in Chittagong, and Gazipur, Narayangonj, Khulna, Rajshahi, Sylhet, and Barisal each had one (DoE, 2018). These stations were installed in urban centers with a population in excess of 500,000. The chemiluminescence method was used for evaluating the NO_2 concentrations in the air. Monthly NO_2 concentration was measured in parts per billion (ppb) (http://case.doe.gov.bd/).

2.4. Indicators of NO_2 concentration

A variety of environmental and anthropogenic parameters influence the degree of tropospheric air pollution in any specific area (Bernard et al., 2001). Existing studies have used various combinations of indicators to examine the association between NO_2 and factors (Cichowicz et al., 2017; Elminir, 2005; Fallmann et al., 2016; Gorai et al., 2015; Kwak et al., 2017; Ryu et al., 2019; Zheng et al., 2019). This study has selected seven indicators based on an extensive literature review. These are: enhanced vegetation index (EVI), wind speed (WS), rainfall, maximum temperature, relative humidity, population, and distance to industrial locations (Table 1). Raster maps of the seven indicators were generated at a 1 km grid to align with the TROPOMI data.

Ryu et al. (2019) indicated that an increase in vegetation cover can reduce NO_2 concentrations. The MOD13A2 EVI product (Didan, 2015) was used in this study to examine this factor. Cloud-free EVI pixels were utilized to obtain monthly means. The local wind speed determines how fast pollutants are transported from their point of origin (Gorai et al., 2015). Monthly WS data were collected from TerraClimate (Abatzoglou et al., 2018). This has a resolution of 2.5 arcmin and is measured in meters per second (m/s). For this study the WS data was converted to kilometers per hour (km/hr). Kwak et al. (2017) concluded that fluctuations in rainfall intensity can either have a positive or negative effect on NO_2, so monthly rainfall data at a spatial resolution of 0.1 arc-degree was acquired from GPM (Huffman et al., 2019) (Table 1). Monthly EVI, WS, and rainfall data over Bangladesh from July 2018 to June 2019 were retrieved using GEE.

Elminir (2005) showed that variations in temperature have an impact on NO_2 pollution while relative humidity is negatively related, so temperature and RH data were collected from BMD (Table 1). The monthly mean of maximum temperature (MMAXT) and RH for all (e.g., 43) stations in Bangladesh were derived using an inverse distance weighted (IDW) function (Childs, 2004).

Industrial activities and vehicular mobility can significantly influence NO_2 pollution, while a dense population means increased anthropogenic forcing (Zhu et al., 2019). 2019 population density data was obtained from WorldPop (www.worldpop.org) (Table 1) and resampled to a 1 km grid using a nearest neighbor resampling method. The concentration of NO_2 is greatest at the source of industrial emissions (Ryu et al., 2019), so all industrial locations within Bangladesh were retrieved from the HOTOSM (Table 1). Distance to industrial locations was subsequently calculated using a Euclidian distance function.

2.5. Linear Mixed Models (LMMs)

Several linear mixed models (LMMs) were developed for this study incorporating VCD of NO_2 as a dependent variable. EVI, rainfall, WS, MMAXT, and RH were employed as dynamic variables, and population density and distance to industries were used as static independent variables. The values of all dependent and independent variables were then grouped by month.

2.5.1. Multicollinearity testing

The existence of multicollinearity among the independent variables needs to be assessed to ensure that values with high standard errors are not produced. As a check, the variance inflation factor (VIF) of all independent variables was estimated (Yu et al., 2015) using an R package (Fox et al., 2018). VIF indicates the degree of variance if the estimated coefficients are inflated by multicollinearity. Values exceeding 2.5 are a cause of concern, while a value >10 indicates multicollinearity (Midi et al., 2010). In this study, the VIF value of all independent variables was estimated to be less than 2.1, indicating that the variables of interest were free from multicollinearity.

2.5.2. Model development

Three types of LMMs — base model, random intercept model, and random intercept and slope model — were developed (Table 2). The base model did not include any independent variables to estimate monthly changes in NO_2. The two other models did incorporate independent variables in their development. The random intercept model allowed intercepts to vary by group (months), while the slopes remained fixed. In contrast, the random intercept and slope model allowed both

the intercepts and slopes to vary by group (i.e., months). Group-specific slopes and intercepts were obtained. The Maximum Likelihood (ML) method was used for coefficient estimation. Heck et al. (2013) recommended the use of the ML method when comparing different models, and where the number of observations is sufficient. An analysis of variance (ANOVA) (Rouder et al., 2016) was conducted to compare the performance of different LMMs. Satterthwaite's *t*-test was used to calculate statistical significance (p values) (Satterthwaite, 1946). An intra-class correlation coefficient (ICC) was also calculated to check how much clustering could be accounted for by each model (Thompson et al., 2012).

Table 2 Structures of the LMM model, employed in this study

Model	**Equation**	
Base model	$y_{ij} = (\alpha_{00} + \alpha_{0j}) + e$	(i)
Random intercept model	$y_{ij} = (\alpha_{00} + \alpha_{0j}) + \beta_1 MMAXT_{ij} + \beta_2 RAIN_{ij} + \beta_3 WS_{ij} + \beta_4 RH_{ij} + \beta_5 EVI_{ij} + \beta_6 POP_i + \beta_7 IND_i + e$	(ii)
Random intercept and slope model	$y_{ij} = (\alpha_{00} + \alpha_{0j}) + (\beta_1 + \mu_{1j}) MMAXT_{ij} + (\beta_2 + \mu_{2j}) RAIN_{ij} + (\beta_3 + \mu_{3j}) WS_{ij} + (\beta_4 + \mu_{4j}) RH_{ij} + \beta_5 EVI_{ij} + \beta_6 POP_i + \beta_7 IND_i + e$	(iii)

where, $y_{ij} = log[\text{VCD of } NO_2]_{ij}$ is log of the tropospheric NO_2 column number density (normalized to 0-1 scale), observed in the i^{th} grid in month j; α_{00} is the fixed intercept and α_{0j} is month specific random intercept; $MMAXT_{ij}$, $RAIN_{ij}$, WS_{ij}, RH_{ij} and EVI_{ij} are monthly mean of maximum temperature, rainfall, WS, RH and EVI observed in the i^{th} grid in month j (normalized to 0-1 scale); $POP_i = log[Population\ density]_i$ is the i^{th} grid (normalized to 0-1 scale); IND_i is the Euclidean distance of the i^{th} grid from nearest industrial activity (normalized to 0-1 scale); β_1~β_7 are fixed slopes for dependent variables; μ_1~μ_7 are random slopes and they are month specific; and e represents residual error.

All data were nested into 12 groups, each group representing an individual month. The primary database was initially used without any kind of data transformation, however some of the models failed to converge due to the high volume of data and the complexity of the models. Sauzet et al. (2013) had recommended the use of LMM in the modelling only when convergence was achieved. To resolve this issue, the highly skewed variables (e.g., NO_2 and population) were log-transformed. Monthly mean rainfall data was converted to mm/day for ease of operation and normalization was

performed to rectify the issue of differing variable scales. Iterative trial and error operations were then conducted until all models converged.

2.5.3. Model hypotheses

The development of the models used multiple hypotheses to explain the relationship between potential factors and NO_2 concentration. The hypotheses of this study were:

1. An abundance of healthy vegetation reduces NO_2 pollution.
2. The mean maximum temperature has a positive correlation. The relationship can also be temporally negative.
3. An increase in the amount of rainfall reduces NO_2 concentration.
4. The pattern of the relationship between wind speed and VCD of NO_2 varies at monthly scale.
5. Relative humidity is negatively correlated with the accumulation of tropospheric NO_2.
6. The higher the population density, the greater the NO_2 concentration is.
7. NO_2 pollution tends to be lower in areas where distance to industrial locations is higher.

3. Results

3.1. Distributions of atmospheric NO_2 and its indicators

Density plots, descriptive statistics of atmospheric NO_2 and the seven indicators are shown in Figure 2. The distribution of two variables (e.g., NO_2 and population density) was positively skewed (Figure 2 a, g). The annual mean of NO_2 was found to be 0.9×10^{-4}mol/m^2 for the whole of Bangladesh. The mean of maximum temperature and relative humidity was 31.05 ^oC and 76.12%, respectively (Figure 2 c, e), indicating that a warm humid climate prevailed during the study period. Win speed variability was high, ranging from 0.36 to 15.84 km/hr (Figure 2 h). EVI ranged from -0.19 to 0.98 with a mean of 0.33 (Figure 2 b). In the case of monthly precipitation, a number of areas received a maximum rainfall of 1.51 mm/hr (Figure 2 d), while some areas did not receive any rainfall. The highest population density was found to be 1682 with a standard deviation of 25.65 people/km^2 (Figure 2 g). A total of 680 industrial locations were recorded, with almost half of these located in the districts of Dhaka and Narayanganj.

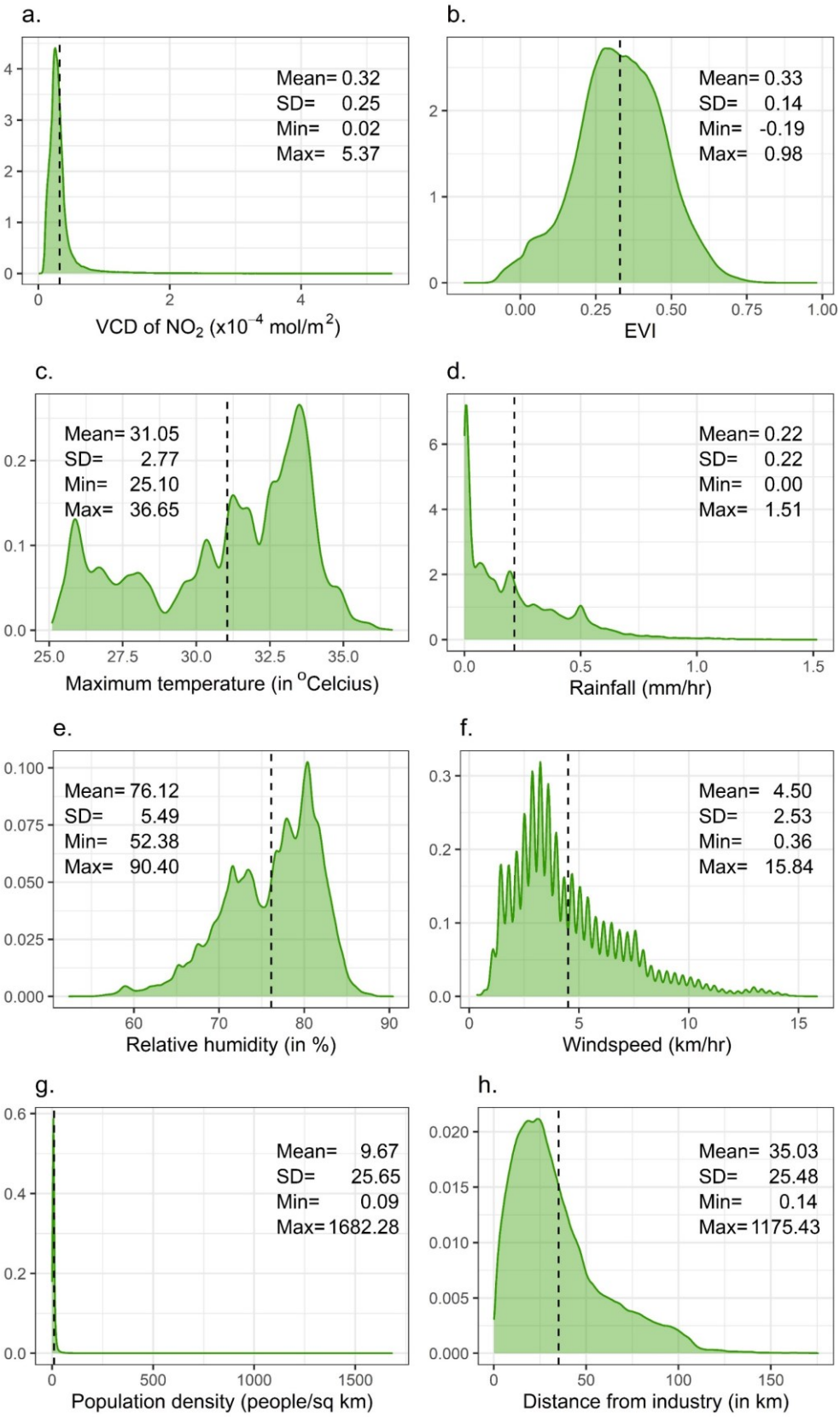

Figure 2 Density plot and descriptive statistics of: (a) VCD of NO_2; (b) Enhanced vegetation index; (c) Mean maximum temperature; (d) Rainfall; (e) Relative humidity; (f) Windspeed; (g) Population density; (h) Industrial locations

3.2. Distribution of NO_2 concentrations

3.2.1. Monthly variation

The spatial variability of NO_2 concentration in Bangladesh in each month (July 2018 to June 2019) is shown in Figure 3. Elevated concentrations were observed between September 2018 and March 2019. The central part of Bangladesh (particularly the capital city of Dhaka and its surroundings) was characterized by higher NO_2 concentrations than the rest of the country. The district-wise tropospheric NO_2 is shown in Figure 4. Pollutant concentrations were greatest in November 2018. The mean concentration was over $0.9 \times 10^{-4} mol/m^2$ in the 5% of the total country area, with the highest value being $5.03 \times 10^{-4} mol/m^2$ in the central region (Dhaka and Narayanganj districts) (Table S1, Figure 4).

During July to August 2018, and in April 2019, however, the NO_2 concentration was $<0.3 \times 10^{-4} mol/m^2$ over more than two-thirds of the country, with only 0.33% of the country recording more than $0.9 \times 10^{-4} mol/m^2$ NO_2 in August 2018. It should be noted that NO_2 concentrations in India influence the atmospheric conditions of western Bangladesh, particularly the Chapai Nawabganj and Rajshahi districts. Chittagong district, the commercial capital of the country, experienced only a moderate level of NO_2 in the atmosphere in March 2019 (Figure 4).

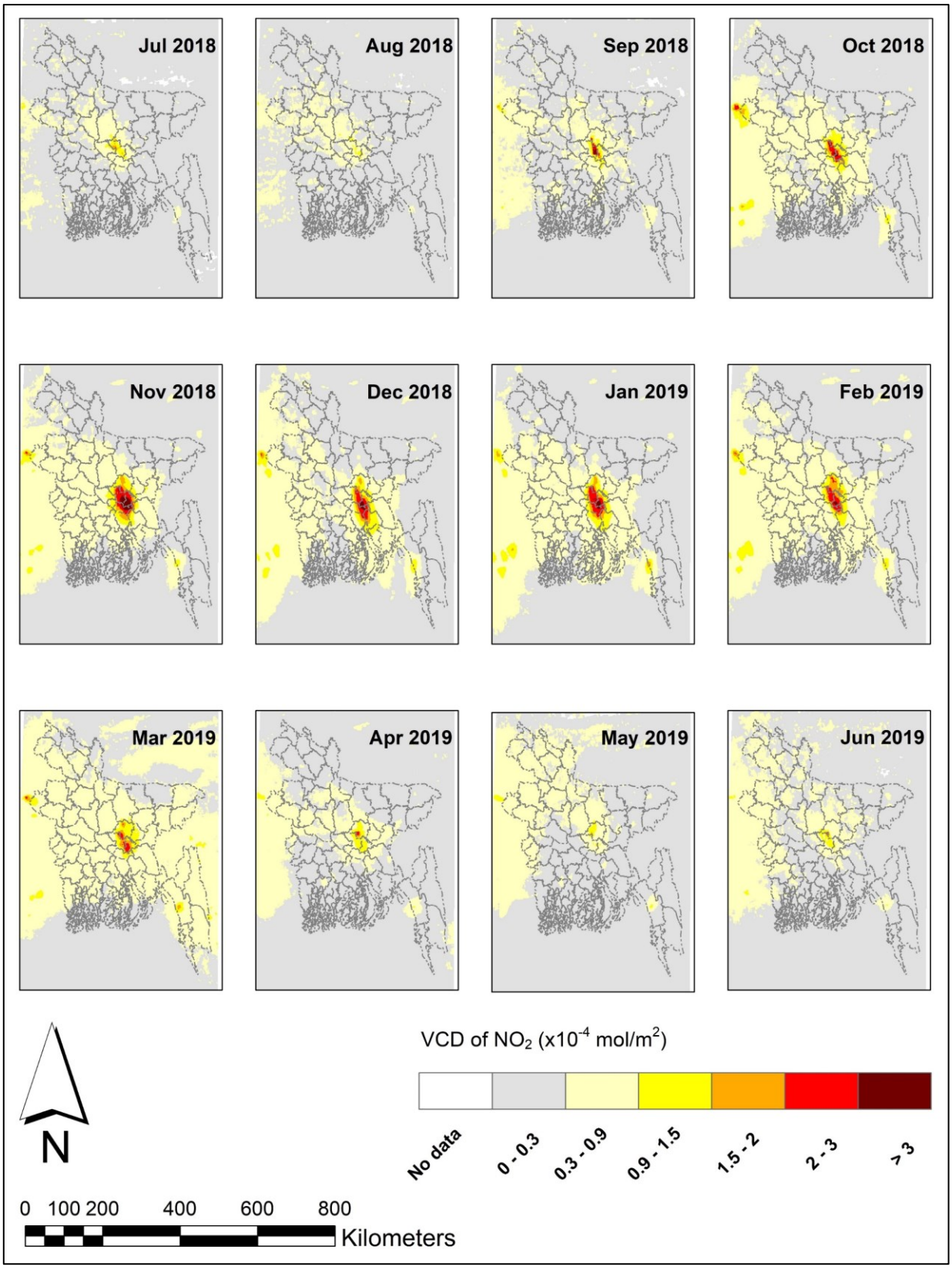

Figure 3 Spatial distribution of tropospheric NO_2 concentration over Bangladesh, 2018-2019

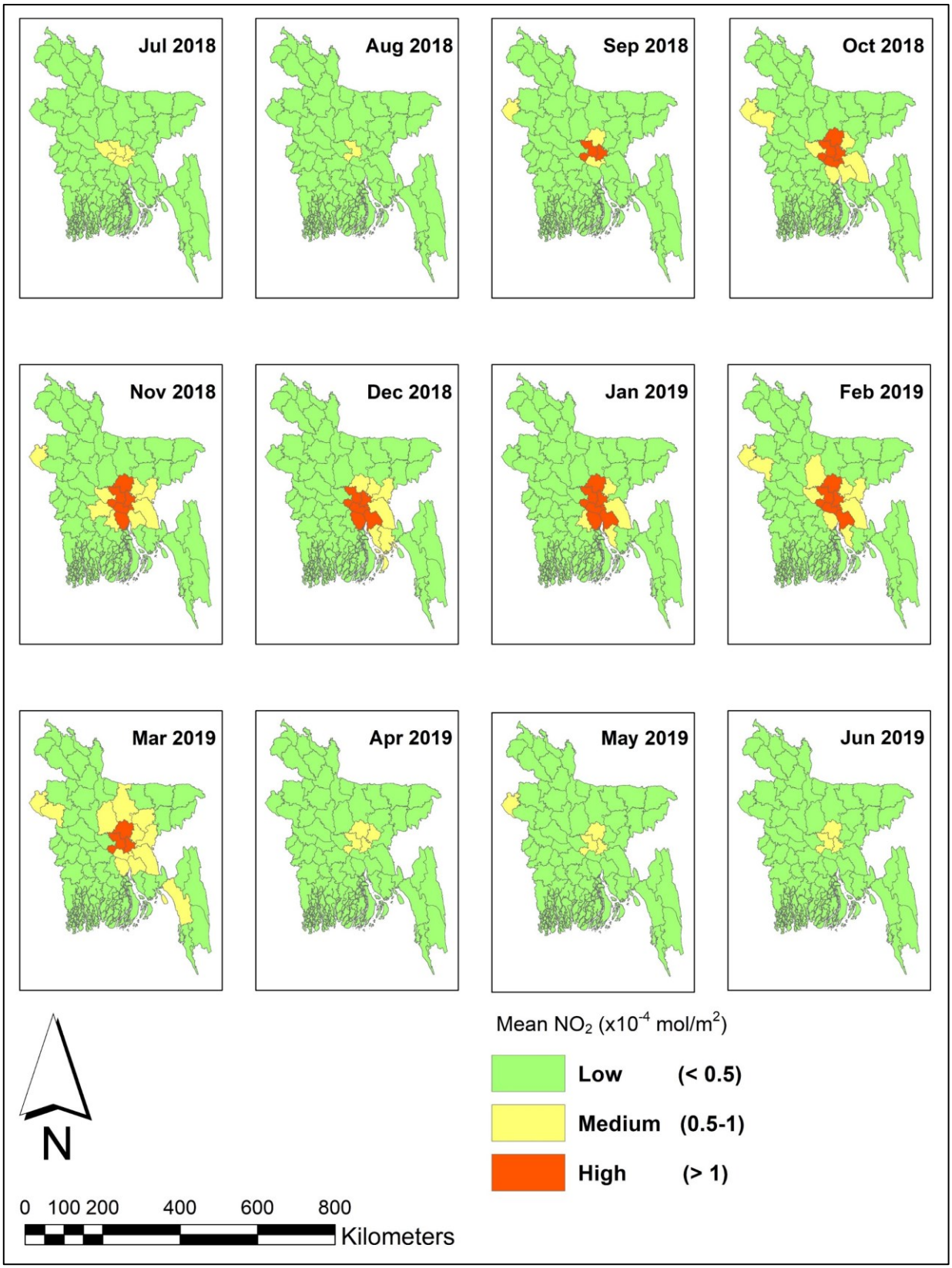

Figure 4 District-wise monthly mean NO_2 concentration

3.2.2. Comparison between satellite and ground-based measurements

Satellite-derived monthly observed NO_2 was plotted against in-situ field data (see Figure 5). This yielded a coefficient of determination (r^2) of 0.67, indicating a good correlation between the two datasets (i.e., in-situ versus satellite). This provides evidence that tropospheric NO_2 can be used as a proxy for ambient NO_2.

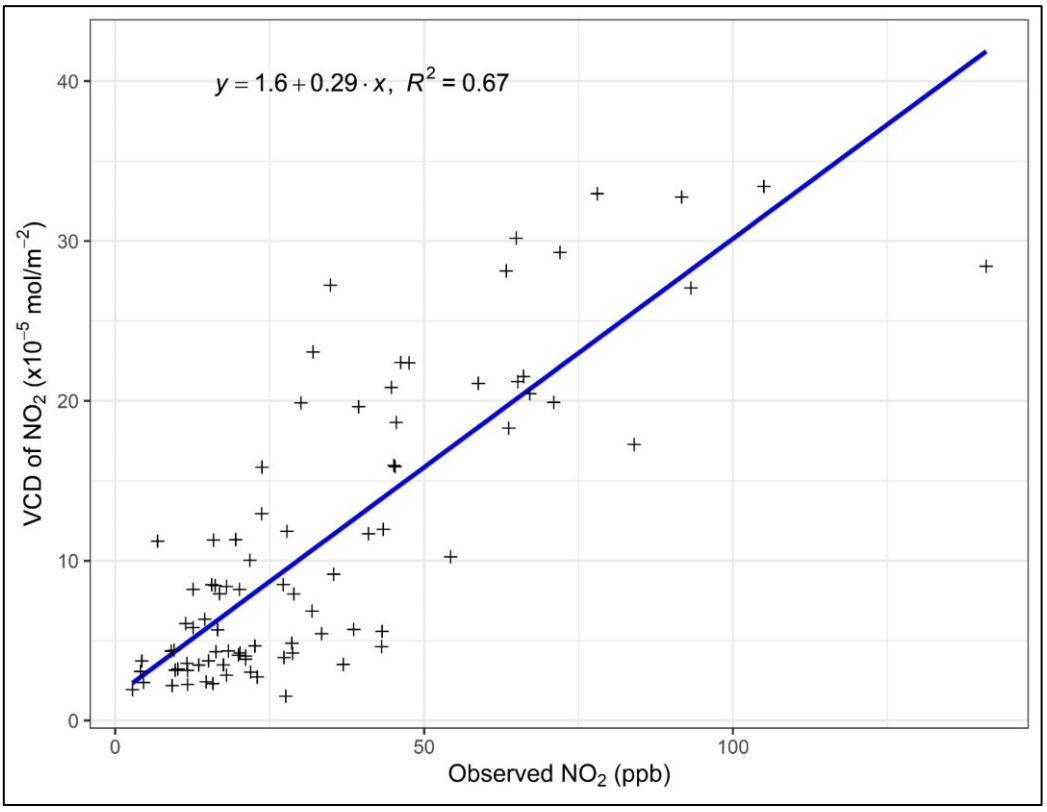

Figure 5 Correlation between in-situ and TROPOMI-based NO_2

3.3. Factors influencing NO_2

A series of linear mixed models (LMMs) were developed to diagnose factors affecting variations in atmospheric NO_2. Table 3 presents a comparative performance of six LMMs. Results show that 14.4% of the variation of the dependent variable could be accounted for by the base model. In contrast, the ICC value increased to 0.174 in Model 2, suggesting that indicators showing clustering effects were more accurate in describing NO_2. Results also showed positive intercept values for all months (Supplementary Table S2), indicating the presence of atmospheric NO_2 across the year. This model did, however, produce a low value for various performance indicators (e.g., p-value) (Table 3). The relationship between monthly atmospheric NO_2 concentration and environmental variables (e.g., MMAXT, RAIN, WS, RH, and EVI), (Supplementary Fig. S2-S6) was examined to identify variables for the random effect models. Supplementary Fig. S2 (a-d) shows the monthly changes in the relationship between NO_2 and environmental factors. Models 3-6 were developed

to allow both intercepts and slopes to vary by month. The interaction between NO_2 and EVI did not vary much by month (Supplementary Fig. S6), so other environmental variables such as RH, MMAXT, RAIN, and WS were added incrementally to model 3-6 Model 6 outperformed all others (see Table 3), as shown by the low residual standard deviation, so Model 6 was employed to determine the effects of various factors on NO_2 distribution in the study area.

Table 3 Performance of different LMM models with ANOVA

Model	ID	Equation	Performance indicators	Indicator values
Base specification	Model 1	y ~ 1 + (1 | Month)	N. parameters	3
			Log-likelihood	1945338
			AIC	-3890670
			BIC	-3890633
			ICC	0.144
			chi-square	
Fixed effect model with all independent variables included	Model 2	y ~ 1 + MMAXT + RAIN + WS + RH + EVI + POP + IND + (1 | Month)	N. parameters	10
			Log-likelihood	2358620
			AIC	-4717221
			BIC	-4717097
			ICC	0.174
			chi-square	826565
			ANOVA test *vs* Model 1	$<2e^{-16}$ ***
Random effect model with only RH slope	Model 3	y ~ 1 + MMAXT + RAIN + WS + RH + EVI + POP + IND + (1 + RH | Month)	N. parameters	12
			Log-likelihood	2389421
			AIC	-4778818
			BIC	-4778670
			ICC	0.805
			chi-square	61601
			ANOVA test *vs* Model 2	$<2e^{-16}$ ***
Random effect model with RH and MMAXT slope	Model 4	y ~ 1 + MMAXT + RAIN + WS + RH + EVI + POP + IND + (1 + RH + MMAXT | Month)	N. parameters	15
			Log-likelihood	2419413
			AIC	-4838796
			BIC	-4838611
			ICC	0.858
			chi-square	59984
			ANOVA test *vs* Model 3	$<2e^{-16}$ ***
Random effect model with RH, MMAXT and RAIN slope	Model 5	y ~ 1 + MMAXT + RAIN + WS + RH + EVI + POP + IND + (1 + RH + MMAXT + RAIN | Month)	N. parameters	19
			Log-likelihood	2436430
			AIC	-4872822
			BIC	-4872588
			ICC	0.807
			chi-square	34034
			ANOVA test *vs* Model 4	$<2e^{-16}$ ***
Random effect model with RH, MAMXT, RAIN and WS slope	Model 6	y ~ 1 + MMAXT + RAIN + WS + RH + EVI + POP + IND + (1 + RH + MMAXT + RAIN + WS | Month)	N. parameters	24
			Log-likelihood	2507269
			AIC	-5014490
			BIC	-5014194
			ICC	0.817
			chi-square	141677
			ANOVA test *vs* Model 5	$<2e^{-16}$ ***

Significant codes: 0 '***' 0.001 '**' 0.01 '*' 0.05 '.' 0.1 ' ' 1

MMAXT = Mean maximum temperature; RAIN = Rainfall amount; WS = Windspeed; RH = Relative humidity; EVI = Enhanced vegetation index; POP = log of population density; IND = Euclidean distance from nearby industrial location

Table 4 summarizes fixed intercept effects of the differing factors. Of the seven independent variables, five were deemed to be statistically significant. Rainfall and WS were flagged as insignificant, indicating that the annual mean value of these parameters had a low level of influence on NO_2. Among the significant variables, both MMAXT and population density had a positive influence, i.e., one unit increase in population density (log-transformed) is likely to increase NO_2 by 3.83% [10*(exp(0.25)*100%-100%)/(10*Max value of log(POP))]. However, the negative coefficients of RH, EVI, and distance to industry indicated that an increase in these variables would decrease NO_2. For instance, one unit increase in EVI could potentially decrease NO_2 by 35.68% [10*(exp(-0.0356)*100%-100%)/Max value of EVI]. EVI represents vegetation condition, so an increase in healthy vegetation is likely to decrease NO_2 pollution.

Table 4 Fixed effects of different factors on NO_2

Term	Coefficient	Standard error	*p*-value	Confidence interval (95%)	
				Low	High
Intercept	0.487	0.033	5.04e-09 ***	0.422	0.553
MMAXT	0.148	0.083	0.098▪	-0.014	0.31
RAIN	0.183	0.329	0.589	-0.462	0.827
WS	-0.054	0.065	0.425	-0.182	0.074
RH	-0.187	0.044	0.0011 **	-0.273	-0.101
EVI	-0.036	0.0004	< 2e-16 ***	-0.036	-0.035
POP	0.250	0.0005	< 2e-16 ***	0.249	0.251
IND	-0.115	0.0004	< 2e-16 ***	-0.115	-0.114

Significant codes: 0 '***' 0.001 '**' 0.01 '*' 0.05 '▪' 0.1 ' ' 1

Estimates of the random effects of the four indicators (RH, MMAXT, rainfall, and WS) on NO_2 is summarized in Table 5. Although annual mean values of rainfall and WS were statistically insignificant (Table 4), the monthly variation was significant and had a month-specific effect on the temporal change in NO_2 (Table 5). Variation in RH and MMAXT was also evident with the deviations of RH positive in four different months (April, May, July, and August), and negative in other months (Table 5).

393 Table 5 Random effects of different factors on NO_2

Term	Parameters	Jul-18	Aug-18	Sep-18	Oct-18	Nov-18	Dec-18	Jan-19	Feb-19	Mar-19	Apr-19	May-19	Jun-19
Intercept	Coefficient	-0.244*	-0.119*	-0.001	0.026*	-0.075*	0.005*	0.038*	-0.006*	-0.018*	0.003	0.212*	0.179*
	Standard error	0.004	0.005	0.006	0.003	0.002	0.002	0.001	0.002	0.002	0.003	0.004	0.006
	Lower bound (95%)	-0.252	-0.130	-0.013	0.020	-0.079	0.002	0.036	-0.010	-0.021	-0.004	0.204	0.166
	Upper bound (95%)	-0.235	-0.109	0.011	0.032	-0.071	0.008	0.041	-0.003	-0.015	0.010	0.221	0.191
RH	Coefficient	0.053*	0.048*	-0.085*	-0.271*	-0.080*	-0.003	-0.074*	-0.045*	0.327*	0.233*	0.021*	-0.125*
	Standard error	0.005	0.004	0.004	0.003	0.002	0.002	0.002	0.003	0.002	0.003	0.004	0.006
	Lower bound (95%)	0.044	0.039	-0.093	-0.276	-0.083	-0.007	-0.078	-0.051	0.324	0.227	0.012	-0.136
	Upper bound (95%)	0.062	0.057	-0.076	-0.265	-0.076	0.001	-0.070	-0.040	0.330	0.239	0.029	-0.113
MMAXT	Coefficient	0.318*	0.154*	0.054*	0.349*	0.561*	-0.452*	-0.308*	0.006*	-0.136*	-0.185*	-0.220*	-0.141*
	Standard error	0.004	0.005	0.006	0.004	0.004	0.003	0.003	0.003	0.003	0.003	0.003	0.004
	Lower bound (95%)	0.311	0.144	0.042	0.342	0.552	-0.458	-0.313	0.000	-0.142	-0.190	-0.225	-0.150
	Upper bound (95%)	0.325	0.164	0.066	0.357	0.569	-0.446	-0.302	0.012	-0.130	-0.180	-0.215	-0.133
RAIN	Coefficient	-0.173*	-0.343*	-0.208*	-0.050*	-2.220*	2.550*	1.670*	0.492*	-0.613*	-0.590*	-0.290*	-0.233*
	Standard error	0.002	0.002	0.003	0.003	0.039	0.045	0.085	0.005	0.010	0.006	0.002	0.002
	Lower bound (95%)	-0.176	-0.346	-0.214	-0.055	-2.300	2.470	1.510	0.482	-0.633	-0.601	-0.294	-0.236
	Upper bound (95%)	-0.169	-0.339	-0.202	-0.045	-2.140	2.640	1.840	0.503	-0.593	-0.578	-0.286	-0.230
WS	Coefficient	-0.053*	-0.079*	0.068*	-0.040*	-0.488*	0.371*	0.425*	0.090*	-0.041*	-0.041*	-0.174*	-0.039*
	Standard error	0.001	0.002	0.002	0.002	0.003	0.002	0.002	0.003	0.002	0.001	0.001	0.002
	Lower bound (95%)	-0.056	-0.082	0.064	-0.044	-0.494	0.367	0.422	0.085	-0.045	-0.044	-0.176	-0.042
	Upper bound (95%)	-0.051	-0.075	0.073	-0.035	-0.482	0.375	0.428	0.095	-0.037	-0.039	-0.172	-0.036

** Significant at 95% confidence level*

394

Table 6 Mixed effects of factors on NO_2 concentration

Month	Intercept	MMAXT	RAIN	WS	RH	EVI	POP	IND
Jul-18	0.244	0.466	0.010	-0.107	-0.134	-0.036	0.250	-0.115
Aug-18	0.368	0.302	-0.160	-0.133	-0.139	-0.036	0.250	-0.115
Sep-18	0.486	0.202	-0.026	0.014	-0.272	-0.036	0.250	-0.115
Oct-18	0.513	0.497	0.133	-0.094	-0.458	-0.036	0.250	-0.115
Nov-18	0.412	0.709	-2.037	-0.542	-0.266	-0.036	0.250	-0.115
Dec-18	0.493	-0.304	2.737	0.317	-0.189	-0.036	0.250	-0.115
Jan-19	0.526	-0.160	1.855	0.371	-0.261	-0.036	0.250	-0.115
Feb-19	0.481	0.154	0.675	0.036	-0.232	-0.036	0.250	-0.115
Mar-19	0.469	0.012	-0.431	-0.095	0.140	-0.036	0.250	-0.115
Apr-19	0.491	-0.037	-0.407	-0.095	0.046	-0.036	0.250	-0.115
May-19	0.700	-0.072	-0.107	-0.228	-0.166	-0.036	0.250	-0.115
Jun-19	0.666	0.007	-0.051	-0.093	-0.312	-0.036	0.250	-0.115

The combined effects of environmental and anthropogenic factors on NO_2 were also examined (see Table 6). Both fixed and random effects were integrated. In this study, the mixed effect is important mostly for MMAXT and RH, because they have shown a significant relationship. The combined effect of MMAXT is evident during the winter months of December and January and monsoon months of April and May, when MMAXT negatively influenced NO_2, although the relationship was positive for other months. RH was significant as a fixed and random effect term (except for December). Examining the mixed effects, it can be noted that RH had a negative influence on NO_2 concentration when the annual average RH was greater than 71%. As the slopes of EVI, population density, and distance from the nearby industry do not vary, their coefficient values are the same for each month (Table 6). The relationship between rainfall and NO_2 also varied throughout the study period with a negative correlation observed during the two monsoon months (July and October) and three winter months (December, January, and February). WS had a negative influence on NO_2 concentration in most months.

4. Discussion

In this study, several LMMs (linear mixed model) were developed to examine the spatiotemporal patterns of atmospheric NO_2 and the factors influencing NO_2 pollution. Results revealed good alignment between satellite-derived and in-situ-based NO_2 values. This appeared primarily due to the fine resolution of the TROPOMI data. A similar result was observed in research undertaken in other areas (Cooper et al., 2020; Goldberg et al., 2021). The mixed-effect analyses showed that the month-specific relationships were statistically significant between NO_2, and the differing climatic variables used. These findings are in accord with Elminir (2005), who reported that ambient temperature, in general, is positively correlated with NO_2 concentration, though the correlation coefficients may vary temporarily. The mean maximum temperature across Bangladesh was less

than 28 °C during December and January, when the temperature was found to be negatively correlated with NO_2. In an examination of the seasonality of air pollution, Cichowicz et al. (2017) found that a lower temperature in the winter months can lead to an increase in NO_2 levels. Work by Kwak et al. (2017) showed that with an increase in rainfall, NO_2 concentration can either increase or decrease. In the present study, results of the combined mixed effect models revealed that rainfall was positively correlated with NO_2 in October but negatively correlated in November. Further investigation revealed the existence of a positive correlation, especially in large cities (e.g., Dhaka and Chittagong) during July when rainfall intensity is usually very high (Shahid, 2011). Kwak et al. (2017) showed that this feature may be related to city traffic volume which tends to increase with heavy rainfall events. In the case of three winter months however (December, January, and February), this variable also had a positive association, despite a lower rainfall intensity. In general an inverse relationship is apparent between precipitation and NO_2 concentration during the summer and rainy seasons. This agrees with Ahmad et al. (2011). The relationship between NO_2 concentration and RH is also in accord with Elminir (2005). The contrasting relationship between RH and NO_2, on the other hand, may be related to the area of interest, data and methods used.

Zhou et al. (2012) observed that the relationship of wind speed with NO_2 can vary, depending on the wind direction. In Bangladesh, the direction of wind fluctuates seasonally (Khan et al., 2004), so its influence on the dispersal of NO_2 varies. In this study, wind speed (as a random term) was found to be significant. The month-specific relationship between wind speed and NO_2 concentration were obvious. The wind speed in winter is relatively low compared to the wind speed during summer (Khan et al., 2004). Low wind speeds result in the slow dispersal of pollutants, and therefore NO_2 can be readily deposited within the emission source area. During winter, when wind speed slightly increases, pollutants in the wind get transported to nearby areas from industrial sites. As a result, wind speed showed a positive correlation during December, January, and February. This finding is in accord with Ryu et al. (2019).

Sahsuvaroglu et al. (2006) detected a high level of NO_2 pollution in the vicinity of industrial establishments in research conducted in Hamilton, Canada. This supports the findings in the current work. The greater the distance of an area from an industry, the lower is the concentration of NO_2 . For instance, NO_2 concentration over Mirpur area of Dhaka city was 3.22 $\times 10^{-4}$mol/m^2 during November 2018. Relocating industries 500 m outward from their current position could reduce the mean monthly concentration of NO_2 in the Mirpur area by 46%. Lamsal et al. (2013) reported a positive association between urban population size and NO_2 concentration in the United States, Europe, China, and India. This also agrees with the current study. The present work noted that population density was positively related to NO_2, and agrees with work by Ryu et al. (2019). This

research also noted that vegetation acts as a reduction factor in regards pollutants such as NO_2. NDVI was used in this previous work. The current work uses EVI, due to the tendency for NDVI to saturate. EVI has a higher degree of sensitivity to the regional variation of green footprints (Zhang et al., 2016). Kumari et al. (2021) observed a negative correlation between NO_2 and EVI which agrees with the current study results; that higher vegetation cover (denoted by EVI) played a strong role in reducing NO_2 pollution. Indications are that a unit increase in EVI could reduce NO_2 concentrations by 35.68%.

5. Conclusion

In this study, space-time variations of tropospheric vertical column density (VCD) of NO_2 over Bangladesh for the period July 2018 to June 2019 were examined using TROPOMI satellite data. The influence of environmental and anthropogenic factors on NO_2 was investigated using linear mixed models (LMMs). Results indicated that the monthly variability in NO_2 concentrations was associated with meteorological factors. Month-specific variability of maximum temperature, relative humidity, rainfall, and wind speed were used in modelling the NO_2 concentration fluctuations. Monthly average maximum temperature and relative humidity were the main factors affecting monthly variations in NO_2 readings. It was observed that an increase in rainfall during the monsoon season could result in either an increase, or a decrease, in observed NO_2. Conversely during the winter, industrial and vehicular emissions seemed to affect the distribution of ambient NO_2, possibly due to the effect of low rainfall. High maximum temperatures can either have a positive or negative relationship with NO_2, and are dependent on the time of year. In general, NO_2 concentrations tended to decrease with an increase in temperature.

This study has a number of limitations. There is likely to be a strong relationship between traffic volume and the accumulation of NO_2. Gridded data on traffic volume throughout Bangladesh are not available, however, so it was not possible to include this variable in the current work. Updated data from DoE air monitoring stations were also not available. Lastly, wind direction as a variable was not considered. Further research is recommended.

Despite the limitations noted above, several suggestions for reducing NO_2 concentrations can be put forward as a result of this work. TROPOMI data can be used, as an alternative to ground-based measurements, to detect the monthly distribution of air pollutants such as NO_2. Using monthly variations in the climatic variables noted, it may become easier to accurately predict NO_2 concentrations in the different regions. Public awareness can be raised, and citizens encouraged to adopt protective measures such as the use of face masks during the months when air pollution is predicted to be a problem. Air is ubiquitous, and is impossible to be contained by any bounding

structure. Emissions from neighboring countries can create a nuisance so transboundary air quality agreements should be in place. A month-specific green tax can be imposed on industries where pollutant emissions are high. Districts with high urbanization rates and high population density normally have high traffic volumes and associated high vehicle emissions. The current study indicates that a decrease in population density could reduce the extent of NO_2 pollution. Decentralization can play two key roles in this regard. Firstly, decentralizing industries and associated activities from major cities could lower population pressure on their surroundings. Secondly, relocating industries from cities would also reduce pollutant concentrations. Increasing the green footprint in urban areas, and use of biophilic designs, can also result in decreased NO_2 pollution. These policy suggestions are applicable not only to Bangladesh, but also to other developing countries that have cities experiencing air pollution problems.

6. References

Abatzoglou, J.T., Dobrowski, S.Z., Parks, S.A., Hegewisch, K.C., 2018. TerraClimate, a high-resolution global dataset of monthly climate and climatic water balance from 1958-2015. Scientific Data 5.

Aggarwal, A., Toshniwal, D., 2019. Detection of anomalous nitrogen dioxide (NO2) concentration in urban air of India using proximity and clustering methods. Journal of the Air & Waste Management Association 69, 805-822.

Ahmad, S.S., Biiker, P., Emberson, L., Shabbir, R., 2011. Monitoring nitrogen dioxide levels in urban areas in Rawalpindi, Pakistan. Water, Air, & Soil Pollution 220, 141-150.

Atkinson, R.W., Butland, B.K., Anderson, H.R., Maynard, R.L., 2018. Long-term concentrations of nitrogen dioxide and mortality. Epidemiology 29, 460-472.

Azkar, M.M.B.I., Chatani, S., Sudo, K., 2012. Simulation of urban and regional air pollution in Bangladesh. Journal of Geophysical Research. Atmospheres 117.

BBS, 2019. Bangladesh Statistics 2019. Bangladesh Bureau of Statistics (BBS), Ministry of Planning, Dhaka, Bangladesh.

Bechle, M.J., Millet, D.B., Marshall, J.D., 2013. Remote sensing of exposure to NO2: Satellite versus ground-based measurement in a large urban area. Atmospheric Environment 69, 345-353.

Bernard, S.M., Samet, J.M., Grambsch, A., Ebi, K.L., Romieu, I., 2001. The potential impacts of climate variability and change on air pollution-related health effects in the United States. Environmental health perspectives 109, 199-209.

Biswal, A., Singh, T., Singh, V., Ravindra, K., Mor, S., 2020. COVID-19 lockdown and its impact on tropospheric NO<inf>2</inf> concentrations over India using satellite-based data. Heliyon 6.

Childs, C., 2004. Interpolating surfaces in ArcGIS spatial analyst. ArcUser, July-September 3235, 569.

Cichowicz, R., Wielgosiński, G., Fetter, W., 2017. Dispersion of atmospheric air pollution in summer and winter season. Environmental Monitoring and Assessment 189.

Cooper, M.J., Martin, R.V., McLinden, C.A., Brook, J.R., 2020. Inferring ground-level nitrogen dioxide concentrations at fine spatial resolution applied to the TROPOMI satellite instrument. Environmental Research Letters 15, 104013.

Davis, R.E., Kalkstein, L.S., 1990. Development of an automated spatial synoptic climatological classification. International Journal of Climatology 10, 769-794.

Didan, K., 2015. MOD13A2 MODIS/Terra Vegetation Indices 16-Day L3 Global 1km SIN Grid V006 [Data set]. NASA EOSDIS Land Processes DAAC.

Dix, B., de Bruin, J., Roosenbrand, E., Vlemmix, T., Francoeur, C., Gorchov-Negron, A., McDonald, B., Zhizhin, M., Elvidge, C., Veefkind, P., 2020. Nitrogen oxide emissions from US oil and gas production: Recent trends and source attribution. Geophysical Research Letters 47, e2019GL085866.

DoE, 2018. Ambient Air Quality in Bangladesh. Department of Environment (DoE), Ministry of Environment, Dhaka, Bangladesh.

Duncan, B.N., Prados, A.I., Lamsal, L.N., Liu, Y., Streets, D.G., Gupta, P., Hilsenrath, E., Kahn, R.A., Nielsen, J.E., Beyersdorf, A.J., Burton, S.P., Fiore, A.M., Fishman, J., Henze, D.K., Hostetler, C.A., Krotkov, N.A., Lee, P., Lin, M., Pawson, S., Pfister, G., Pickering, K.E., Pierce, R.B., Yoshida, Y., Ziemba, L.D., 2014. Satellite data of atmospheric pollution for U.S. air quality applications: Examples of applications, summary of data end-user resources, answers to FAQs, and common mistakes to avoid. Atmospheric Environment 94, 647-662.

El-Assi, W., Salah Mahmoud, M., Nurul Habib, K., 2017. Effects of built environment and weather on bike sharing demand: a station level analysis of commercial bike sharing in Toronto. Transportation 44, 589-613.

Elminir, H.K., 2005. Dependence of urban air pollutants on meteorology. Science of the Total Environment 350, 225-237.

ESA, 2018. TROPOMI Level 2 Nitrogen Dioxide total column products. Version 01. European Space Agency (ESA).

Eskes, H., Van Geffen, J., Boersma, F., Eichmann, K., Apituley, A., Pedergnana, M., Sneep, M., Veefkind, J.P., Loyola, D., 2019. 5P TROPOMI Level-2 Product User Manual - Nitrogen Dioxide - Document Library - Sentinel Online.

Fallmann, J., Forkel, R., Emeis, S., 2016. Secondary effects of urban heat island mitigation measures on air quality. Atmospheric Environment 125, 199-211.

Fox, J., Weisberg, S., Price, B., Adler, D., Bates, D., Baud-Bovy, G., Bolker, B., Ellison, S., Firth, D., Friendly, M., 2018. Package 'car'.

Gelman, A., Hill, J., 2006. Data analysis using regression and multilevel/hierarchical models. Cambridge university press.

Georgoulias, A.K., Van Der, R.A.J., Stammes, P., Folkert Boersma, K., Eskes, H.J., 2019. Trends and trend reversal detection in 2 decades of tropospheric NO2 satellite observations. Atmospheric Chemistry and Physics 19, 6269-6294.

563 Goldberg, D.L., Anenberg, S.C., Kerr, G.H., Mohegh, A., Lu, Z., Streets, D.G., 2021. TROPOMI NO2 in
564 the United States: A detailed look at the annual averages, weekly cycles, effects of temperature, and
565 correlation with surface NO2 concentrations. Earth's future 9, e2020EF001665.
566 Gorai, A.K., Tuluri, F., Tchounwou, P.B., Ambinakudige, S., 2015. Influence of local meteorology and
567 NO2 conditions on ground-level ozone concentrations in the eastern part of Texas, USA. Air
568 Quality, Atmosphere and Health 8, 81-96.
569 Gorelick, N., Hancher, M., Dixon, M., Ilyushchenko, S., Thau, D., Moore, R., 2017. Google Earth Engine:
570 Planetary-scale geospatial analysis for everyone. Remote Sensing of Environment 202, 18-27.
571 Heck, R.H., Thomas, S.L., Tabata, L.N., 2013. Multilevel and longitudinal modeling with IBM SPSS.
572 Routledge.
573 Herron-Thorpe, F., Lamb, B., Mount, G., Vaughan, J., 2010. Evaluation of a regional air quality forecast
574 model for tropospheric NO2 columns using the OMI/Aura satellite tropospheric NO2 product.
575 Atmospheric Chemistry and Physics 10, 8839.
576 Huffman, G.J., Stocker, E.F., Bolvin, D.T., Nelkin, E.J., Tan, J., 2019. GPM IMERG Final Precipitation L3
577 1 month 0.1 degree x 0.1 degree V06, Greenbelt, MD. Goddard Earth Sciences Data and
578 Information Services Center (GES DISC)
579
580 Islam, M.N., Ali, M.A., Islam, M.M., 2019. Spatiotemporal Investigations of Aerosol Optical Properties
581 Over Bangladesh for the Period 2002–2016. Earth Systems and Environment 3, 563-573.
582 Islam, M.S., Tusher, T.R., Roy, S., Rahman, M., 2020. Impacts of nationwide lockdown due to COVID-19
583 outbreak on air quality in Bangladesh: a spatiotemporal analysis. Air Quality, Atmosphere &
584 Health, 1-13.
585 Juhos, I., Makra, L., Tóth, B., 2008. Forecasting of traffic origin NO and NO2 concentrations by Support
586 Vector Machines and neural networks using Principal Component Analysis. Simulation Modelling
587 Practice and Theory 16, 1488-1502.
588 Khan, M., Iqbal, M., Mahboob, S., 2004. A wind map of Bangladesh. Renewable energy 29, 643-660.
589 Kumari, M., Somvanshi, S.S., Zubair, S., 2021. Estimation of Air Pollution Using Regression Modelling
590 Approach for Mumbai Region, Maharashtra, India, Remote Sensing and GIScience. Springer, pp.
591 229-247.
592 Kurata, M., Takahashi, K., Hibiki, A., 2020. Gender differences in associations of household and ambient
593 air pollution with child health: Evidence from household and satellite-based data in Bangladesh.
594 World Development 128, 104779.
595 Kwak, H.-Y., Ko, J., Lee, S., Joh, C.-H., 2017. Identifying the correlation between rainfall, traffic flow
596 performance and air pollution concentration in Seoul using a path analysis. Transportation research
597 procedia 25, 3552-3563.
598 Lamsal, L., Martin, R., Parrish, D., Krotkov, N., 2013. Scaling relationship for NO2 pollution and urban
599 population size: a satellite perspective. Environmental science & technology 47, 7855-7861.

Lee, H., Liu, Y., Coull, B., Schwartz, J., Koutrakis, P., 2011. A novel calibration approach of MODIS AOD data to predict PM 2.5 concentrations. Atmospheric Chemistry and Physics 11, 7991-8002.

Lee, H.J., Koutrakis, P., 2014. Daily ambient NO2 concentration predictions using satellite ozone monitoring instrument NO2 data and land use regression. Environmental science & technology 48, 2305-2311.

Li, T., Wang, Y., Yuan, Q., 2020. Remote Sensing Estimation of Regional NO2 via Space-Time Neural Networks. Remote Sensing 12, 2514.

Liu, C., Henderson, B.H., Wang, D., Yang, X., Peng, Z.-r., 2016. A land use regression application into assessing spatial variation of intra-urban fine particulate matter (PM2. 5) and nitrogen dioxide (NO2) concentrations in City of Shanghai, China. Science of The Total Environment 565, 607-615.

Lorente, A., Boersma, K., Eskes, H., Veefkind, J., Van Geffen, J., de Zeeuw, M., van der Gon, H.D., Beirle, S., Krol, M., 2019. Quantification of nitrogen oxides emissions from build-up of pollution over Paris with TROPOMI. Scientific reports 9, 1-10.

Magezi, D.A., 2015. Linear mixed-effects models for within-participant psychology experiments: an introductory tutorial and free, graphical user interface (LMMgui). Frontiers in psychology 6, 2.

Melamed, M.L., Schmale, J., von Schneidemesser, E., 2016. Sustainable policy—Key considerations for air quality and climate change. Current opinion in environmental sustainability 23, 85-91.

Midi, H., Sarkar, S.K., Rana, S., 2010. Collinearity diagnostics of binary logistic regression model. Journal of Interdisciplinary Mathematics 13, 253-267.

Mullick, M.R.A., Nur, R.M., Alam, M.J., Islam, K.A., 2019. Observed trends in temperature and rainfall in Bangladesh using pre-whitening approach. Global and planetary change 172, 104-113.

Nemet, G.F., Holloway, T., Meier, P., 2010. Implications of incorporating air-quality co-benefits into climate change policymaking. Environmental Research Letters 5, 014007.

Novotny, E.V., Bechle, M.J., Millet, D.B., Marshall, J.D., 2011. National satellite-based land-use regression: NO2 in the United States. Environmental science & technology 45, 4407-4414.

Omrani, H., Omrani, B., Parmentier, B., Helbich, M., 2020. Spatio-temporal data on the air pollutant nitrogen dioxide derived from Sentinel satellite for France. Data in brief 28, 105089.

Rahman, M.M., Mahamud, S., Thurston, G.D., 2019. Recent spatial gradients and time trends in Dhaka, Bangladesh, air pollution and their human health implications. Journal of the Air & Waste Management Association 69, 478-501.

Rahman, M.S., Azad, M.A.K., Hasanuzzaman, M., Salam, R., Islam, A.R.M.T., Rahman, M.M., Hoque, M.M.M., 2020. How air quality and COVID-19 transmission change under different lockdown scenarios? A case from Dhaka city, Bangladesh. Science of The Total Environment, 143161.

Rana, M.M., Khan, M.H., 2020. Trend Characteristics of Atmospheric Particulate Matters in Major Urban Areas of Bangladesh. Asian Journal of Atmospheric Environment (AJAE) 14.

Rouder, J.N., Engelhardt, C.R., McCabe, S., Morey, R.D., 2016. Model comparison in ANOVA. Psychonomic Bulletin & Review 23, 1779-1786.

637 Ryu, J., Park, C., Jeon, S.W., 2019. Mapping and Statistical Analysis of NO2 Concentration for Local
638 Government Air Quality Regulation. Sustainability 11, 3809.
639 Sadia, H.-E., Jeba, F., Uddin, M.Z., Salam, A., 2019. Sensitivity study of plant species due to traffic emitted
640 air pollutants (NO 2 and PM 2.5) during different seasons in Dhaka, Bangladesh. SN Applied
641 Sciences 1, 1377.
642 Sahsuvaroglu, T., Arain, A., Kanaroglou, P., Finkelstein, N., Newbold, B., Jerrett, M., Beckerman, B.,
643 Brook, J., Finkelstein, M., Gilbert, N.L., 2006. A land use regression model for predicting ambient
644 concentrations of nitrogen dioxide in Hamilton, Ontario, Canada. Journal of the Air & Waste
645 Management Association 56, 1059-1069.
646 Salam, A., Hossain, T., Siddique, M., Alam, A.S., 2008. Characteristics of atmospheric trace gases,
647 particulate matter, and heavy metal pollution in Dhaka, Bangladesh. Air Quality, Atmosphere &
648 Health 1, 101.
649 Satterthwaite, F.E., 1946. An approximate distribution of estimates of variance components. Biometrics
650 bulletin 2, 110-114.
651 Sauzet, O., Wright, K., Marston, L., Brocklehurst, P., Peacock, J., 2013. Modelling the hierarchical structure
652 in datasets with very small clusters: a simulation study to explore the effect of the proportion of
653 clusters when the outcome is continuous. Statistics in medicine 32, 1429-1438.
654 Shah, V., Jacob, D.J., Li, K., Silvern, R.F., Zhai, S., Liu, M., Lin, J., Zhang, Q., 2020. Effect of changing
655 NO x lifetime on the seasonality and long-term trends of satellite-observed tropospheric NO 2
656 columns over China. Atmospheric Chemistry and Physics 20, 1483-1495.
657 Shahid, S., 2011. Trends in extreme rainfall events of Bangladesh. Theoretical and applied climatology 104,
658 489-499.
659 Shikwambana, L., Mhangara, P., Mbatha, N., 2020. Trend analysis and first time observations of sulphur
660 dioxide and nitrogen dioxide in South Africa using TROPOMI/Sentinel-5 P data. International
661 Journal of Applied Earth Observation and Geoinformation 91, 102130.
662 Spicer, C.W., Kenny, D.V., Ward, G.F., Billick, I.H., 1993. Transformations, lifetimes, and sources of NO2,
663 HONO, and HNO3 in indoor environments. Air & Waste 43, 1479-1485.
664 Thompson, D.M., Fernald, D.H., Mold, J.W., 2012. Intraclass correlation coefficients typical of cluster-
665 randomized studies: estimates from the Robert Wood Johnson Prescription for Health projects. The
666 Annals of Family Medicine 10, 235-240.
667 Tzortziou, M., Parker, O., Lamb, B., Herman, J.R., Lamsal, L., Stauffer, R., Abuhassan, N., 2018.
668 Atmospheric Trace Gas (NO2 and O3) variability in South Korean coastal waters, and implications
669 for remote sensing of coastal ocean color dynamics. Remote Sensing 10, 1587.
670 ul-Haq, Z., Rana, A.D., Tariq, S., Mahmood, K., Ali, M., Bashir, I., 2018. Modeling of tropospheric NO2
671 column over different climatic zones and land use/land cover types in South Asia. Journal of
672 Atmospheric and Solar-Terrestrial Physics 168, 80-99.

673 Vîrghileanu, M., Săvulescu, I., Mihai, B.-A., Nistor, C., Dobre, R., 2020. Nitrogen Dioxide (NO2) Pollution
674 Monitoring with Sentinel-5P Satellite Imagery over Europe during the Coronavirus Pandemic
675 Outbreak. Remote Sensing 12, 3575.
676 Wang, Y., Tao, J., Cheng, L., Yu, C., Wang, Z., Chen, L., 2019. A Retrieval of Glyoxal from OMI over
677 China: Investigation of the Effects of Tropospheric NO2. Remote Sensing 11, 137.
678 WHO, 2014. 7 million premature deaths annually linked to air pollution. World Health Organization
679 Wu, S., Huang, B., Wang, J., He, L., Wang, Z., Yan, Z., Lao, X., Zhang, F., Liu, R., Du, Z., 2021.
680 Spatiotemporal mapping and assessment of daily ground NO2 concentrations in China using high-
681 resolution TROPOMI retrievals. Environmental Pollution 273, 116456.
682 Xu, J., Xie, H., Wang, K., Wang, J., Xia, Z., 2020. Analyzing the spatial and temporal variations in
683 tropospheric NO 2 column concentrations over China using multisource satellite remote sensing.
684 Journal of Applied Remote Sensing 14, 014519.
685 Yu, H., Jiang, S., Land, K.C., 2015. Multicollinearity in hierarchical linear models. Social science research
686 53, 118-136.
687 Zhang, T., Gong, W., Wang, W., Ji, Y., Zhu, Z., Huang, Y., 2016. Ground level PM2. 5 estimates over
688 China using satellite-based geographically weighted regression (GWR) models are improved by
689 including NO2 and enhanced vegetation index (EVI). International journal of environmental
690 research and public health 13, 1215.
691 Zheng, C., Zhao, C., Li, Y., Wu, X., Zhang, K., Gao, J., Qiao, Q., Ren, Y., Zhang, X., Chai, F., 2018. Spatial
692 and temporal distribution of NO2 and SO2 in Inner Mongolia urban agglomeration obtained from
693 satellite remote sensing and ground observations. Atmospheric environment 188, 50-59.
694 Zheng, Z., Yang, Z., Wu, Z., Marinello, F., 2019. Spatial Variation of NO2 and Its Impact Factors in China:
695 An Application of Sentinel-5P Products. Remote Sensing 11, 1939.
696 Zhou, Y., Brunner, D., Hueglin, C., Henne, S., Staehelin, J., 2012. Changes in OMI tropospheric NO2
697 columns over Europe from 2004 to 2009 and the influence of meteorological variability.
698 Atmospheric Environment 46, 482-495.
699 Zhu, Y., Xie, J., Huang, F., Cao, L., 2020. Association between short-term exposure to air pollution and
700 COVID-19 infection: Evidence from China. Science of the total environment, 138704.
701 Zhu, Y., Zhan, Y., Wang, B., Li, Z., Qin, Y., Zhang, K., 2019. Spatiotemporally mapping of the relationship
702 between NO2 pollution and urbanization for a megacity in Southwest China during 2005–2016.
703 Chemosphere 220, 155-162.